Functional and structural characterization of two Bacillus megaterium nitroreductases biotransforming the herbicide mesotrione.

Louis Carles, Pascale Pascale Besse, P. Besse-Hoggan Besse-Hoggan, Muriel Joly, Armelle Vigouroux, Solange Moréra, Isabelle Batisson

▶ **To cite this version:**

Louis Carles, Pascale Pascale Besse, P. Besse-Hoggan Besse-Hoggan, Muriel Joly, Armelle Vigouroux, Solange Moréra, et al.. Functional and structural characterization of two Bacillus megaterium nitroreductases biotransforming the herbicide mesotrione.. Biochemical Journal, 2016, 473 (10), pp.1443-1453. 10.1042/BJ20151366 . hal-01457189

HAL Id: hal-01457189
https://hal.science/hal-01457189v1

Submitted on 11 Dec 2023

HAL is a multi-disciplinary open access archive for the deposit and dissemination of scientific research documents, whether they are published or not. The documents may come from teaching and research institutions in France or abroad, or from public or private research centers.

L'archive ouverte pluridisciplinaire **HAL**, est destinée au dépôt et à la diffusion de documents scientifiques de niveau recherche, publiés ou non, émanant des établissements d'enseignement et de recherche français ou étrangers, des laboratoires publics ou privés.

Functional and structural characterization of two *Bacillus megaterium* nitroreductases biotransforming the herbicide mesotrione

Louis Carles*†, Pascale Besse-Hoggan‡§, Muriel Joly*†, Armelle Vigouroux‖, Solange Moréra‖ and Isabelle Batisson*†[1]

*Clermont Université, Université Blaise Pascal, Laboratoire Microorganismes: Génome et Environnement (LMGE), F-63000 Clermont-Ferrand, France
†Centre National de la Recherche Scientifique (CNRS), UMR 6023, LMGE, TSA 60026, CS 60026, 63178 Aubière Cedex, France
‡Clermont Université, Université Blaise Pascal, Institut de Chimie de Clermont-Ferrand (ICCF), F-63000 Clermont-Ferrand, France
§CNRS, UMR 6296, ICCF, TSA 60026, CS 60026, 63178 Aubière Cedex, France
‖Institute for Integrative Biology of the Cell (I2BC), CNRS, Commissariat à l'Énergie Atomique et aux Énergies Alternatives (CEA), Université Paris-Sud, Université Paris-Saclay, F-91198, Gif-sur-Yvette, France

Mesotrione is a selective herbicide belonging to the triketone family, commonly used on maize cultures since 2003. A mesotrione-transforming *Bacillus megaterium* Mes11 strain isolated from an agricultural soil was used as a model to identify the key enzymes initiating the biotransformation of this herbicide. Two enzymes (called NfrA1 and NfrA2/YcnD) were identified, and functionally and structurally characterized. Both belong to the NfsA FRP family of the nitro-FMN reductase superfamily (type I oxygen-insensitive nitroreductase) and show optimal pH and temperature of 6–6.5 and 23–25 °C, respectively. Both undergo a Ping Pong Bi Bi mechanism, with NADPH and NADPH/NADH as cofactors for NfrA1 and NfrA2/YcnD, respectively. It is interesting that both can also reduce various nitro compounds including pesticides, antibiotics, one prodrug and 4-methylsulfonyl-2-nitrobenzoic acid, one of the mesotrione metabolites retrieved from the environment. The present study constitutes the first identification of mesotrione-transforming enzymes. These enzymes (or their corresponding genes) could be used as biomarkers to predict the capacity of ecosystems to transform mesotrione and assess their contamination by both the parent molecule and/or the metabolites.

Key words: *Bacillus megaterium*, biotransformation, mesotrione herbicide, nitroreductase enzyme.

INTRODUCTION

A new generation of herbicides, both more specific and used on crops at lower doses, has recently appeared on the market [1,2]. However, the reduction in agronomic doses is not necessarily linked to a decrease in leaching, contamination and potential (eco)toxicity because novel molecules and their transformation products can be more toxic than those previously used [3]. We focused our study on the β-triketone herbicide mesotrione, commonly used to treat maize culture since the prohibition of the use of atrazine in 2003 in the European Union. Mesotrione's fate has already been well studied in crops, soil and water [4]. Its water solubility and sorption coefficient values make this compound relatively mobile and bioavailable in soils, allowing biotransformation processes [5,6]. The main metabolites found in mesotrione-contaminated environments are 4-methylsulfonyl-2-nitrobenzoic acid (MNBA) and 2-amino-4-methylsulfonyl benzoic acid (AMBA) [7].

The mesotrione biotransformation pathways are well conserved among several bacterial mesotrione-transforming strains isolated from various environments such as *Bacillus* sp. 3B6 [8] and *Pantoea* sp. 5B12 [9], isolated from cloud water, *Bacillus pumilus* HZ-2 isolated from an anaerobic wastewater treatment plant [10], *Bacillus megaterium* Mes11 [11] and *Bradyrhizobium* sp. SR1 [12], isolated from an agricultural soil or a laboratory strain of *Escherichia coli* (ATCC 11303) [9]. Two pathways have been described, each one being major or minor according to the strain: the first involves reduction of the nitro group of mesotrione into free or cyclized hydroxylamino intermediates and hydrolysis of the β-diketone bond, leading to the final accumulation of AMBA; the second involves an oxidative cleavage of the mesotrione and a reduction of the nitro group, leading to the MNBA intermediate, and finally transformation into AMBA [13]. Although mesotrione transformation pathways have been well studied, no genes and/or enzymes involved in its biotransformation have been described so far. A recent proteomic study of *B. megaterium* Mes11 revealed a network of mesotrione-adaptative proteins directly linked to nitroreductase (NR) enzymes, possibly involved in its biotransformation into AMBA [14]. This result agreed with the chemical structures of the observed intermediate metabolites, corresponding to the reduction of the mesotrione nitro group into an amino moiety.

NR enzymes are known for their ability to reduce nitro-aromatic compounds *via* one- or two-electron transfer by type II and type I NRs, respectively [15,16]. The type II NRs contain FMN or FAD as cofactor and their activity is oxygen-sensitive. They catalyse the one-electron reduction of a nitro compound, forming a nitro anion radical. In the presence of oxygen, this radical undergoes futile cycling, resulting in the production of superoxide anions and regeneration of the parent nitro compound [17]. The type I NRs (oxygen-insensitive NRs) are NAD(P)H-dependent, FMN-binding proteins. They catalyse the sequential two-electron reduction of the nitro group into a nitroso intermediate which rapidly undergoes reduction to

Abbreviations: AMBA, 2-amino-4-methylsulfonyl benzoic acid; DAD, diode array detector; FLD, fluorescence detector; MNBA, 4-methylsulfonyl-2-nitrobenzoic acid; MPD, (4*S*)-2-methyl-2,4-pentanediol; NPB, native purification buffer; NR, nitroreductase; qPCR, quantitative PCR.

[1] To whom correspondence should be addressed (email isabelle.batisson@univ-bpclermont.fr).

© 2016 Authors; published by Portland Press Limited

Table 1 Name and sequence of primers used in this study

The *B. megaterium*-targeted gene names are indicated, as well as the family and superfamily of their corresponding protein.

PCR primer name	Gene name	Protein family	Protein superfamily	Nucleotide sequence (5′–3′)	Annealing temperature (°C)	Amplicon size (bp)	Reference or source
A Forward	*ntr*A	Arsenite oxidase	Nitro-FMN reductase	ATGAGCGTATTAGATATTATTAAAGCC	55	558	The present study
A Reverse				YTAACGATACCAAATCGTTTTATCTTG			
B Forward	*nfr*A1	NfsA FRP	Nitro-FMN reductase	ATGAACTCAGTTATTGAAACGATTTTA	55	747	The present study
B Reverse				TTATTTCTTRTTAAATCCTTGCTTTTC			
C Forward	*ntr*C	Nitroreductase 1	Nitro-FMN reductase	ATGACTATAAAAGACTTTAACGAAATTG	55	624	The present study
C Reverse				TTATTTCCAAGTCGTAACCGTATTG			
C1 Forward	*cbi*Y	Arsenite oxidase	Nitro-FMN reductase	ATGACGATTATYTCACAGYTAAAAG	55	567	The present study
C1 Reverse				TTACAGCCATGTTGTTTTTTCTGTAAAC			
D Forward	*yod*C	Nitroreductase 1	Nitro-FMN reductase	ATGACAAAAGATTTTTTTGATGTGGTAA	55	609	The present study
D Reverse				TTAAATCCAAGTTGTAACTTGATCYAATG			
E Forward	*yfk*O	NfsB-like nitroreductase	Nitro-FMN reductase	ATGAACMATACAGATAARAAACAAGAA	55	666	The present study
E Reverse				YTATTTTAYCCACTGTACAACTTGATC			
F Forward	*nfr*A2 (*ycn*D)	NfsA FRP	Nitro-FMN reductase	ATGAATGAAGCAATTCGTACAATTC	55	735	The present study
F Reverse				TTATTCGAATTTAAATCCTTGTTTTTCAAG			
G Forward	*ntr*G	Nitroreductase 4	Nitro-FMN reductase	ATGGGTTTTTYAGATAAATTATTTGATAAATC	55	642	The present study
G Reverse				TTATTTAAATACTTTTACACGTTCASTTAG			
H Forward	*ydg*I	Nitroreductase 1	Nitro-FMN reductase	ATGACACMAACAAAAACACTAAAC	55	639	The present study
H Reverse				TTATCTAAATTGAGCTACTTTTTCGATTG			
T7 Forward	[b]	[b]	[b]	TAATACGACTCACTATAGGG	51	Insert dependent	pEXP5-CT/TOPO TA
T7 Term Reverse				ATCCGGATATAGTTCCTCCTTTC			Expression Kit (Invitrogen)
NfrA1 Forward[a]	*nfr*A1	[b]	[b]	CCGAATGATGAGCAGACGAA	57	94	The present study
NfrA1 Reverse[a]				GTGTCTTGGCGTTTGCCATT			
NfrA2 Forward[a]	*nfr*A2 (*ycn*D)	[b]	[b]	CAACAGTTGCAGCAGAATCAC	57	96	The present study
NfrA2 Reverse[a]				CCGGTAAATCGAGCAGTTCA			
BAC338 Forward[a]	16S rRNA	[b]	[b]	ACTCCTACGGGAGGCAG	57	180	[18]
515 Reverse[a]				ATTACCGCGGCTGCTGGCA			

[a]qPCR primers.
[b]Not applicable.

hydroxylamino and amino intermediates from electron pairs of NAD(P)H [15,16].

The aim of the present study was to identify and functionally and structurally characterize the initial mesotrione-transforming enzymes. As the mesotrione transformation by *B. megaterium* Mes11 strain was observed in aerobic conditions, with the formation of hydroxylamino intermediates and AMBA, we hypothesize that type I NR activity could be responsible for the first step of mesotrione biotransformation. We have thus identified the type I Mes11 NR enzymes and tested their ability to transform mesotrione.

EXPERIMENTAL

Bacterial strains and chemicals

The mesotrione-transforming strain *B. megaterium* Mes11 was isolated from an agricultural soil as previously described [11]. *E. coli* BL21(DE3) (pLys) cells were purchased from Thermo Scientific. Mesotrione, dinoseb, imidacloprid (Pestanal, purity 99.9 %), MNBA (purity >99 %), parathion (Pestanal, purity 99.0 %), parathion-methyl (Pestanal, purity 99.8 %), fluazinam (Pestanal, purity 98.5 %), nitrofurazone (Fluka), chloramphenicol, 5-(1-aziridinyl)-2,4-dinitrobenzamide (CB1954) (purity >98 %), thiamethoxam (Pestanal, purity 99.7 %) and metronidazole (Fluka, purity >98 %) were purchased from Sigma–Aldrich.

PCR amplification of the NR-coding genes

The extraction of genomic DNA from *B. megaterium* Mes11 was performed using the QIAamp DNA Mini Kit (Qiagen) following the manufacturer's recommendations. Primers for PCR amplification of NR-coding genes were designed using primer basic local alignment search tool (BLAST) (Table 1) and obtained from Eurofins. The PCRs were performed in a total volume of 50 μl, containing 200 μM of each dNTP, 0.2 μM of each primer, and 1× PCR buffer containing 2.5 mM $MgCl_2$, 0.3 unit of Taq polymerase (Eurobio) and 50 ng of genomic DNA. The PCRs were performed in a Mastercycler (Eppendorf) as follows: initial denaturation at 95 °C for 5 min, 30 cycles of denaturation at 94 °C for 1 min, primer annealing at 55 °C for 1 min and elongation at 72 °C for 1 min, and a final extension step at 72 °C for 10 min.

Complete nucleotide sequences of the NR genes *ydg*I, *ntr*G, *nfr*A2/*ycn*D, *yfk*O, *yod*C, *cbi*Y, *ntr*C, *nfr*A1 and *ntr*A of *B. megaterium* Mes11 were deposited in GenBank under accession numbers KT008914–KT008922, respectively.

Expression and purification of NRs in *E. coli*

The amplification products were cloned into the expression vector pEXP5-CT/TOPO. The expression of the recombinant NRs was performed in *E. coli* BL21 Star (DE3) pLysS cells as described by Bers et al. [19], with some modifications. The expression was realized by induction with 1 mM IPTG and incubation at 37 °C for 5 h for all NRs, except NtrA and NtrG, which

© 2016 Authors; published by Portland Press Limited

Table 2 Crystallographic data and refinement parameters

Values for the highest resolution shell are in parentheses.

Protein (PDB code)	*B. megaterium* NrfA1 (5HDJ)	*B. megaterium* NfrA2/YcnD (5HEI)
Space group	$P2_12_12_1$	$P2_1$
Cell parameters (Å, °)	$a = 56.9$, $b = 87.2$, $c = 93.6$	$a = 64.4$, $b = 158.2$, $c = 103.9$, $\beta = 102.2$
Number of dimers in the asymmetrical unit	1	4
Resolution (Å)	48–1.89 (2.01–1.89)	50–2.84 (3.01–2.84)
Number of observed reflections	255507 (33513)	129776 (19322)
Number of unique reflections	36741 (5655)	44446 (6781)
R_{sym} (%)	21.8 (101.7)	24.5 (103.1)
Completeness (%)	99.4 (96.4)	97.3 (92.6)
$I/\sigma I$	7.52 (1.65)	4.88 (1.3)
$CC_{1/2}$[a]	99.1 (65.8)	97 (59)
R_{cryst} (%)	17.43	20.3
R_{free} (%)[b]	20.6	24.7
RMSD bond (Å)	0.01	0.008
RMSD angle (°)	1.03	1.05
Average B (Å^2) protein, FMN cofactor, solvent	26.9, 15, 32.4	60.5, 54.4, 43.2

[a] $CC_{1/2}$ = percentage of correlation between intensities from a random half-dataset [21].
[b] Of the data 5 % were set aside for free calculation of the R factor.

were induced at 4 °C for 72 h. The size of the recombinant proteins was checked using the SDS/PAGE molecular mass standards, broad range (Bio-Rad Laboratories). The recombinant *E. coli* BL21 Star (DE3) pLysS (pEX-CT_NR) strains were cultured in 1 litre of LB overnight at 37 °C under agitation (200 rev./min). After centrifugation of the culture (15 min at 3400 ***g***), the pellet was resuspended in either 5 ml of native equilibration buffer (Thermo Fisher Scientific) for kinetic studies or 50 mM Tris/HCl, pH 8, 20 mM imidazole and 500 mM NaCl for structural studies. The concentrated cell suspension was lysed twice in a One Shot Cell disrupter (Constants Systems) under 2.6 kbar (1 kbar = 100 000 kPa) pressure. Cell debris were eliminated by centrifugation (20000 ***g*** for 1 h at 4 °C) and the supernatant was loaded on a HisPur Ni^{2+}-nitrilotriacetate (Ni-NTA) Superflow agarose column for protein purification (Thermo Fisher Scientific), as recommended by the manufacturer. For structural studies, enzyme elution was performed using 50 mM Tris/HCl, pH 8, 300 mM imidazole and 500 mM NaCl. The fractions containing the enzyme were loaded on a gel-filtration column (HiLoad 26/60 Superdex 200 prep grade, GE Healthcare) equilibrated with 50 mM Tris/HCl, pH 8, and 150 mM NaCl. NfrA1 and NfrA2/YcnD enzymes were concentrated at 7.3 and 9.4 mg/ml, respectively, and stored at − 80 °C.

Crystallization and structure determination

Crystallization conditions (Qiagen kits) were screened in sitting-drop vapour-diffusion experiments using a nanodrop cartesian robot (proteomic solutions) at 293 K. Crystals were obtained in 15 % (w/v) PEG 4000 and 0.1 M Mes, pH 6.5, for NfrA1 and in 3.5 M ammonium sulfate, 5 % (4*S*)-2-methyl-2,4-pentanediol (MPD) and 0.1 M Mes, pH 6.5, for NfrA2/YcnD. They were transferred into the mother solution supplemented with 25 % (w/v) PEG 400 and 30 % glucose, respectively, before being flash-frozen in liquid nitrogen. Diffraction data for NfrA1 and NfrA2/YcnD crystals were collected at 100 K on the PROXIMA 1 beamline (Synchrotron SOLEIL). Intensities were integrated using an XDS program [20] and data quality was assessed using the correlation coefficient $CC_{1/2}$ (Table 2).

Solvent content analysis using CCP4 indicated the presence of one dimer or four dimers in the asymmetrical unit of *B. megaterium* NfrA1 or NfrA2/YcnD crystals, respectively. The structural determination was performed by molecular replacement with Phaser [22], using the co-ordinates of the *B. subtilis* NfrA1 dimer (PDB code 3N2S [23]) and the *B. subtilis* YcnD (also named NfrA2) dimer (PDB code 1ZCH [24]) as a search model for *B. megaterium* NfrA1 and NrfA2/YcnD structures, respectively. Both enzyme models were refined using non-crystallographic symmetry (NCS) restraints and total least squares (TLS) using Buster [25]. Electron density maps were evaluated using the Crystallographic Object-Oriented Toolkit (COOT) [26].

The atomic co-ordinates and structure factors of NfrA1 and NfrA2/YcnD Mes11 have been deposited in the PDB (http://www.rcsb.org) under accession codes 5HDJ and 5HEI.

NR enzyme assays

The reduction activity for the nitro group of each of the nine NRs was first checked in the presence of 100 μM mesotrione or MNBA prepared in native purification buffer (NPB), pH 7.5 (5 mM NaH_2PO_4 and 500 mM NaCl), 400 μM NAD(P)H and 1.8 μM enzyme at 28 °C. The reaction was stopped after 1 h by the addition of HCl (final concentration 6 %, v/v). The concentration of remaining mesotrione or MNBA was then determined using HPLC.

The optimal pH and temperature for activity of mesotrione-reducing enzymes were determined as described above for pH varying from 2.9 to 8.2 (fixed temperature: 25 °C) and for temperatures varying from 22.5 °C to 47.7 °C (fixed pH: 6).

The reaction mechanism and kinetic constants were determined by monitoring the NAD(P)H oxidation rate at 340 nm [NAD(P)H molar absorption coefficient $\varepsilon = 6220\ M^{-1}\cdot cm^{-1}$] at the optimal pH and temperature of enzymes with a Cary 300 UV-Vis spectrophotometer (Agilent). The reactions were carried out in NPB with fixed concentrations of substrates (0, 50, 100 and 400 μM mesotrione or MNBA) adding different concentrations of cofactor [0, 100, 200, 300 and 400 μM NAD(P)H] and 0.43 μM NfrA1 or 1.78 μM NfrA2/YcnD. The innate levels of NAD(P)H oxidase activity of both enzymes were determined using enzymatic assays without substrate for each incubation condition. The stability of NAD(P)H was checked using assays without enzymes. The initial velocity was determined in the linear

© 2016 Authors; published by Portland Press Limited

phase when <10 % of the substrate has depleted (i.e. <2 min in our assays). The double-reciprocal plots of the initial velocity of both enzymes with each substrate and cofactor were realized and a re-plot (secondary plot) of the *y*-axis intercepts against MNBA concentrations or cofactor (NADPH and NADH) concentrations was used to estimate the kinetic parameters (see Table 4). The reaction mechanism was determined using Lineweaver–Burk plots that resulted from assays with MNBA as substrate and NADPH and NADH as cofactor for NfrA1 and NfrA2/YcnD, respectively (see Supplementary Figure S2).

The quantitative time-course transformation of mesotrione and MNBA and mass balance calculation were carried out at the optimal pH and temperature as described above, in the presence of 2.4 μM NfrA1 and NfrA2/YcnD. The capacity of Mes11 NfrA1 and NfrA2/YcnD to reduce various nitro substrates [used as soluble: 400 μM of substrate except for dinoseb and parathion-methyl (200 μM), parathion (80 μM) and fluazinam (5 μM)] was tested as described above at the optimal pH and temperature, in the presence of 1.8 μM NfrA1 and NfrA2/YcnD. The reaction was monitored using HPLC after 1 h of incubation.

*Nfr*A1 and *nfr*A2/*ycn*D gene expression levels in *B. megaterium* Mes11

The Mes11 cultures (20 ml) were produced at 25 °C under agitation (150 rev./min) in Tryptone soya (TS) medium supplemented or not with 0.15 mM mesotrione (in triplicate). The mesotrione concentrations were measured using HPLC as described below. Cultures (1 ml) were sampled and DNA/RNA extraction was carried out as described by Dugat-Bony et al. [27]. The DNase treatments (twice) and reverse transcription were performed using the DNaseI kit (Invitrogen) and the SuperScript III Reverse Transcriptase kit (Invitrogen) with Random Primers (Invitrogen), respectively. The quantitative PCRs (qPCRs) were performed in a total reaction volume of 15 μl containing 7.5 μl of MasterMix, 0.3 μM of each primer (see Table 1) and 1 μl of ten-fold diluted cDNA. The qPCR was carried out in white qPCR 96-well plates (Eurogentec) using the MESA GREEN qPCR MasterMix Plus for SYBR Assay Low ROXkit (Eurogentec), in a Realplex^2 epgradient S Mastercycler (Eppendorf) as follows: initial denaturation at 95 °C for 5 min, 40 cycles of denaturation at 95 °C for 30 s, primer annealing at 57 °C for 15 s and elongation at 72 °C for 20 s. The 16S rRNA gene was used to normalize the results using primers described by Borrel et al. [18].

Analyses of the nitro compounds tested and their metabolites

The analyses of the nitro compounds were monitored by HPLC on an Agilent Series 1100 chromatograph, equipped with diode array detector (DAD) and fluorescence detectors (FLDs) and a reverse-phase column (Zorbax Eclipse XDB-C_{18}, 3.5 μm, 75 mm × 4.6 mm). The mobile phase was composed of acetonitrile (solvent A) and water or acidified water (H_3PO_4, 0.01, % v/v, pH 2.9) (solvent B) in various gradients according to the compound tested (Table 3). Each sample was analysed twice.

^{1}H NMR analyses were performed at 25 °C at 500.134 MHz on an Avance 500 Bruker spectrometer (Bruker Biospin) equipped with a triple-resonance (^{1}H, ^{13}C, ^{15}N) inverse probe with tubes of 5-mm diameter containing 600 μl of sample (540 μl of sample with 60 μl of 5 mM tetradeuterated sodium trimethylsilylpropionate); water was suppressed by a classic two-phase-shifted pulse-saturation sequence (double-pulsed field gradient echo sequence WATERGATE) according to Durand et al. [13].

LC–ESI–MS analyses were performed according to previously described conditions [28] on a Waters/Micromass LC-quadrupole (Q)-TOF (Micromass), equipped with an orthogonal geometry Z-spray ion source. The crude supernatants were harvested (5 min at 13 000 ***g***) before LC–MS analyses and directly injected into the LC–MS system, with no further treatment. The analyses were carried out in positive mode for mesotrione samples and negative mode for MNBA ones.

RESULTS AND DISCUSSION

Identification of NR mesotrione-transforming candidates in the *B. megaterium* Mes11 strain

The first step of the project was to screen the NR-coding genes in available genomes of *B. megaterium* for subsequent identification of homologue candidates in the *B. megaterium* Mes11 strain. The UniProt Knowledge Base/SwissProt databases (online version, 28 November 2013) were used to collect NR nucleic acid sequences in the three *B. megaterium* genomes available (GenBank accession numbers CP003017, CP001982 and CP001983), revealing a total of nine genes, all of which coded for oxygen-insensitive type I NRs. Several of these type I NRs were shown to reduce nitro-aromatic compounds [29], suggesting a potential involvement of some of them in the transformation of mesotrione. The NR homologous genes of these three strains were aligned and a set of degenerated primers was designed for each gene (see Table 1). These primer pairs allowed us to successfully amplify the nine homologous NR-coding genes from the genomic DNA of *B. megaterium* Mes11.

To test the Mes11 NRs' activity against mesotrione, the corresponding genes were cloned into a pEXP5-CT/TOPO expression vector and the subsequent His-tagged enzymes were purified. The SDS/PAGE analysis revealed monomer sizes of NRs ranging from 21.9 kDa to 29.3 kDa, which is consistent with their theoretical molecular mass (see Supplementary Figure S1). Of the nine Mes11 NRs tested, only two were capable of reducing the nitro group of mesotrione: NfrA1 (EC 1.5.1.38) and NfrA2/YcnD (EC 1.5.1.39). It is interesting that these two enzymes were also the only ones able to accept MNBA, a metabolite formed as traces (∼60 μM, monitored by ^{1}H NMR) by the second and minor pathway previously described [13,28], during mesotrione (10 mM) biotransformation by Mes11.

Characterization of NfrA1 and NfrA2/YcnD from *B. megaterium* Mes11

Structural analysis

The NfrA1 and NfrA2/YcnD Mes11 enzymes belong to the NfsA FRP family of the oxygen-insensitive type I NR, as well as their closest homologues, *B. subtilis* NfrA1 (PDB code 3N2S) and YcnD/NfrA2 (PDB code 1ZCH), sharing 59.44 % and 68.16 % of amino acid sequence identity, respectively. Mes11 NfrA1 and NfrA2/YcnD both exhibit 40.82 % of amino acid sequence identity. The protein structures of NfrA1 and NfrA2/YcnD Mes11 (Figures 1A and 1B), determined by X-ray crystallography at 1.89 Å and 2.84 Å (1 Å = 0.1 nm) resolution adopt the same topology as that of these family members for the monomeric and dimeric forms, which is the active form in solution in accordance with results from gel-filtration chromatography (molecular mass estimates at 58.6 and 56.1 kDa, respectively). Each monomer of 249 amino acids for NfrA1 and 246 residues for NfrA2/YcnD binds an FMN cofactor in the crevice at the dimer interface, and exhibits a three-layer $\alpha\beta\alpha$-sandwich central domain and an

© 2016 Authors; published by Portland Press Limited

Table 3 HPLC conditions for the nitro-compound analyses

Nitro compounds	Solvent	Gradient	Wavelengths	Flow (ml/min)
Mesotrione, MNBA	A: acidified water (H_3PO_4, 0.01 % v/v; pH 2.9) B: acetonitrile	0–1 min 2 % B, 1–8 min 2–70 % B linear, 8–9 min 70–100 % B, 9–9.3 min 100–2 % B, 9.3–10.3 min 2 % B	$\lambda = 254$ nm (DAD) $\lambda_{ex} = 220$ nm $\lambda_{em} = 430$ nm (FLD)	1
Mesotrione, MNBA	A: acidified water (H_3PO_4, 0.01 % v/v; pH 2.9) B: acetonitrile	Longer gradient for metabolite identification 0–5 min 5 % B, 5–30 min 5–70 % B linear, 30–32 min 70–100 % B, 32–33 min 100–5 % B, 33–35 min 5 % B	$\lambda = 254$ nm (DAD) $\lambda_{ex} = 220$ nm $\lambda_{em} = 430$ nm (FLD)	1
Parathion-methyl, parathion, dinoseb	A: acidified water (H_3PO_4, 0.01 % v/v; pH 2.9) B: acetonitrile	0–1 min 2 % B, 1–8 min 2–100 % B linear, 8–10 min 100 % B, 10–11 min100–2 % B, 11–12 min 2 % B	$\lambda = 270$ nm (DAD)	1
Chloramphenicol, thiamethoxam, imidaclopride	A: acidified water (H_3PO_4, 0.01 % v/v; pH 2.9) B: acetonitrile	0–1 min 2 % B, 1–10 min 2–50 % B linear, 10–11 min 50–100 % B, 11–12 min 100–2 % B	$\lambda = 254$ and 270 nm (DAD)	1
CB1954	A: acidified water (H_3PO_4, 0.01 % v/v; pH 2.9) B: acetonitrile	0–1 min 10 % B, 1–19 min 10–30 % B linear, 19–20 min 30–100 % B, 20–20.3 min 100–10 % B	$\lambda = 330$ nm (DAD)	1
Metronidazole	A: acidified water (H_3PO_4, 0.01 % v/v; pH 2.9) B: acetonitrile	0–1 min 3 % B, 3–10 min 3–90 % B linear, 10–11 min 90 % B, 11–11.3 min 90–3 % B, 11.3–12 min 3%	$\lambda = 230$ nm (DAD)	0.8 (35 °C)
Nitrofurazone	A: water B: acetonitrile	0–1 min 2 % B, 1–10 min 2–50 % B linear, 10–11 min 50–100 % B, 11–12 min 100–2 % B	$\lambda = 375$ nm (DAD)	1
Fluazinam	A: water B: acetonitrile	0–1 min 2 % B, 1–8 min 2–70 % B linear, 8–9 min 70–100 % B, 9–9.3 min 100–2 % B, 9.3–10.3 2 % B	$\lambda = 270$ nm (DAD)	0.8

excursion domain. Structural comparison of the four dimers of *B. megaterium* and *B. subtilis* NfrA1 and NfrA2/YcnD leads to RMSDs of between 1 Å and 1.28 Å over 244 Cα atoms per monomer, and reveals a very similar FMN-binding pocket, in which the FMN was superimposed with its *re* face accessible to the substrate. Of the 13 residues of *B. megaterium* NfrA1 involved in FMN binding *via* polar or hydrophobic contacts up to 3.7 Å, nine are conserved (Figure 1C). Despite several attempts, we did not obtain crystal structures of each enzyme as a complex with a NAD(P)H cofactor or with the substrates used in the present study.

Determination of the optimal pH and temperature for mesotrione transformation by NfrA1 and NfrA2/YcnD

The optimal mesotrione transformation activity of the two enzymes was observed at pH 6–6.5 (Figure 2A). It was below the optimal pH observed for the *B. subtilis* homologues NfrA1 and YcnD/NfrA2, which were pH 7 and 8, respectively [24,31]. It is interesting that both Mes11 enzymes conserved at least 60–80 % of their activities at pH values between 5 and 7.5. This is a relatively broad range of pH compared with other NRs, for which activity often sharply declines above or below the optimal pH [32,33]. The maximum mesotrione transformation activity of NfrA1 and NfrA2/YcnD occurred at around 23–25 °C (Figure 2B), which is similar to NfrA1 and YcnD/NfrA2 of *B. subtilis* [24,31]. Both Mes11 NRs conserved at least 60 % of their maximal activity between 4 and 42 °C, NfrA2/YcnD having almost maximal activity on a broad range of temperatures (4–35 °C). These results could make this enzyme suitable for biotechnological applications requiring catalytic activity at low temperature or medicinal applications at human body temperature, such as activation of bioreductive prodrugs or antibiotics [34].

Reaction mechanism, kinetic parameters and substrate specificity of NfrA1 and NfrA2/YcnD

The mesotrione-transformation activity tests showed that NfrA1 uses NADPH as a cofactor. It is interesting that NfrA2/YcnD uses either NADPH or NADH, although the preference for NADPH over NADH is commonly described for the other NfsA FRP family members. The determination of the reaction mechanism and kinetic parameters of Mes11 NfrA1 and NfrA2/YcnD was carried out with mesotrione and MNBA by following the NAD(P)H oxidation rate at 340 nm. The innate levels of NAD(P)H oxidase activity revealed by enzymatic assays without substrate were checked and, under our conditions (short time), did not interfere with the determination of kinetic parameters. The correlation between the concentrations of NAD(P)H oxidized and each substrate reduced was checked for both enzymes. Spearman's correlation coefficients (r) were as follows: (i) NfrA1: NADPH and mesotrione ($r = 0.9976$, $P < 0.001$), NADPH and MNBA ($r = 0.9980$, $P < 0.001$); (ii) NfrA2/YcnD: NADH and mesotrione ($r = 0.9678$, $P < 0.001$), NADH and MNBA ($r = 0.9946$, $P < 0.001$). The analysis of the Lineweaver–Burk plots allowed us to identify a Ping Pong Bi Bi mechanism for NfrA1 and NfrA2/YcnD with MNBA substrate (see Supplementary Figure S2). Similar results were obtained with mesotrione as the electron acceptor (not shown). This mechanism is commonly evidenced for other nitro-FMN reductase superfamily members, including *B. subtilis* NfrA1 and

© 2016 Authors; published by Portland Press Limited

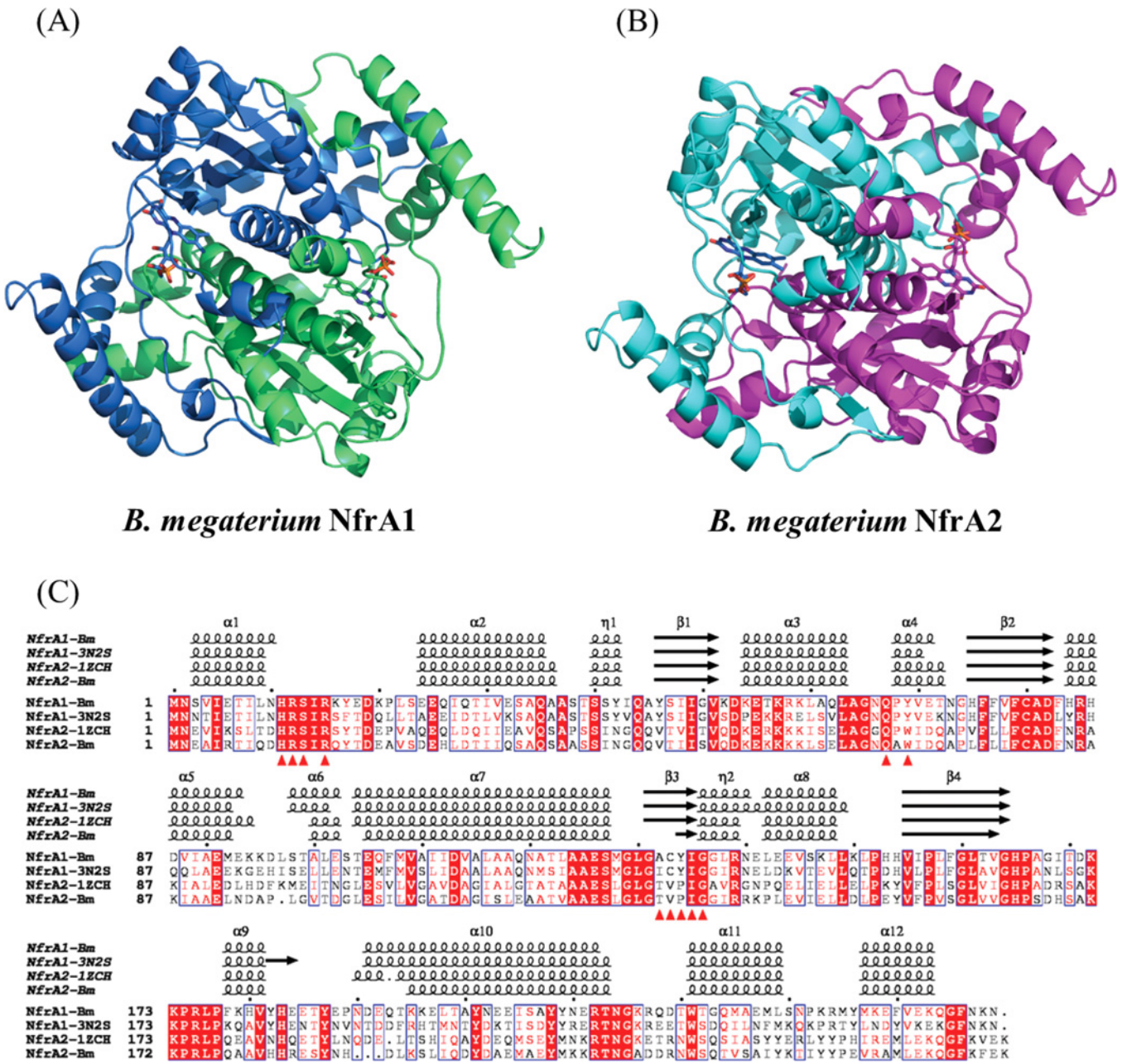

Figure 1 Representations of the *B. megaterium* dimers

Ribbon representation of (**A**) NfrA1 and (**B**) NfrA2/YcnD. FMN cofactors are shown as sticks. (**C**) Structure-based sequence alignment of *B. megaterium* NfrA1 and NfrA2/YcnD with *B. subtilis* NfrA1 (PDB code 3N2S) and NfrA2 (PDB code 1ZCH). Secondary structure elements are labelled and indicated by coils for α-helices, arrow for β-strands and h for short 3_{10} helices. Similar residues are in red and identical residues are shown as white letters on a red background. The positions of *B. megaterium* NfrA1 residues involved in FMN binding are indicated by red triangles. The figure was created using ESPript [30].

YcnD/NfrA2, and *E. coli* NfsA (homologue of Mes11 NfrA1) [24,31,35]. Such a mechanism involves entry of NAD(P)H into the active site, reduction of the tightly bound FMN in $FMNH_2$, dissociation of $NAD(P)^+$ and subsequent reduction of the nitro-aromatic compound by $FMNH_2$. This mechanism was also confirmed by enzyme assays in the presence of free FMN (results not shown). In this case, the nitro-reduction activities were not observed with mesotrione or MNBA as the electron acceptor, suggesting a competitive inhibitory effect of free FMN against nitro compounds. The secondary plots obtained from the Lineweaver–Burk plot data led us to determine kinetic parameters of NfrA1 and NfrA2/YcnD (Table 4). The Michaelis–Menten constant, K_m, of NADPH for NfrA1 and NfrA2/YcnD, and of NADH for NfrA2/YcnD, are about 7, 10 and 28-fold higher than those obtained for their *B. subtilis* homologues NfrA1 and YcnD/NfrA2, respectively [24,31]. The MNBA turnover rate (k_{cat}) was higher for NfrA1 than for NfrA2/YcnD, whereas NfrA2/YcnD showed a 4-fold higher mesotrione turnover rate than NfrA1. The k_{cat}/K_m values for Mes11 NRs indicate less efficiency of NfrA2/YcnD compared with NfrA1 for the reduction of mesotrione or MNBA in the presence of NADPH as the electron donor. In contrast, NfrA2/YcnD showed better efficiency than

© 2016 Authors; published by Portland Press Limited

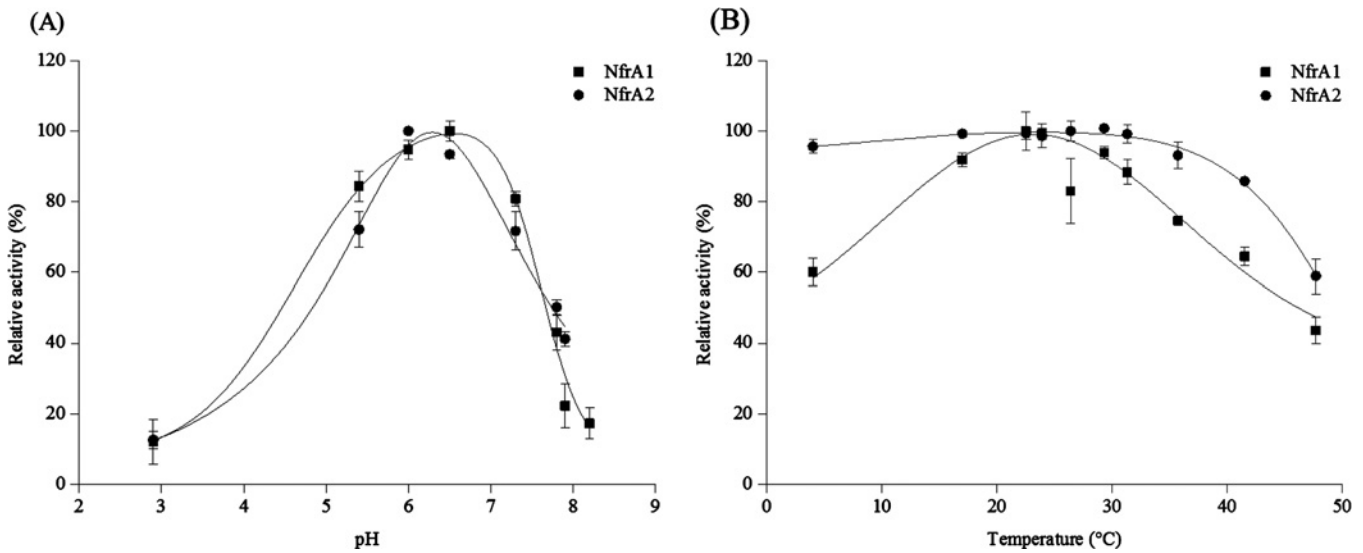

Figure 2 The pH and temperature profiles of mesotrione-transformation activity

The (**A**) pH and (**B**) temperature profiles of mesotrione-transformation activity for NfrA1 and NfrA2/YcnD, determined after 1 h of incubation. Relative activity was determined using HPLC analysis as the decrease in the mesotrione chromatogram peak area. Results are reported as means ± S.D. ($n = 3$). Curves of NfrA1 (pH), NfrA2/YcnD (pH), NfrA1 (temperature) and NfrA2/YcnD (temperature) were fitted using OriginPro 8 software (OriginLab) with asymmetrical double sigmoidal function (Asym2Sig, $R^2 = 0.9793$), Lorentz's function ($R^2 = 0.9878$), Gauss's function ($R^2 = 0.9696$) and the Chesler–Cram peak function (CCE, $R^2 = 0.9553$), respectively.

Table 4 Kinetic parameters for *B. megaterium* Mes11 NfrA1 and NfrA2/YcnD nitroreductases

The NAD(P)H constants were estimated with MNBA as electron acceptor. The NfrA1 and NfrA2/YcnD constants for mesotrione and MNBA were estimated with [a]NADPH or [b]NADH as the electron donor. The results are reported as the means ± S.D. ($n = 3$).

	K_m (μM)	V_{max} (μM/min)	k_{cat} (/min)	k_{cat}/K_m (/μM per min)
NfrA1				
NADPH	28.49 ± 0.31	24.45 ± 1.83	57.32 ± 4.28	1.92 ± 0.03
Mesotrione[a]	24.57 ± 3.78	11.28 ± 0.42	6.61 ± 0.25	0.27 ± 0.04
MNBA[a]	217.87 ± 32.10	25.45 ± 1.92	59.66 ± 4.51	0.28 ± 0.02
NfrA2/YcnD				
NADPH	42.60 ± 23.76	28.52 ± 5.04	9.74 ± 1.72	0.38 ± 0.06
Mesotrione[a]	327.65 ± 64.42	65.55 ± 15.06	22.38 ± 5.14	0.07 ± 0.01
MNBA[a]	101.10 ± 17.82	26.98 ± 2.86	9.21 ± 0.98	0.09 ± 0.03
NADH	176.31 ± 8.70	23.67 ± 2.66	13.28 ± 1.50	0.07 ± 0.01
Mesotrione[b]	67.99 ± 6.81	44.33 ± 4.87	24.87 ± 2.73	0.37 ± 0.01
MNBA[b]	37.45 ± 6.23	23.79 ± 2.54	13.35 ± 1.43	0.36 ± 0.02

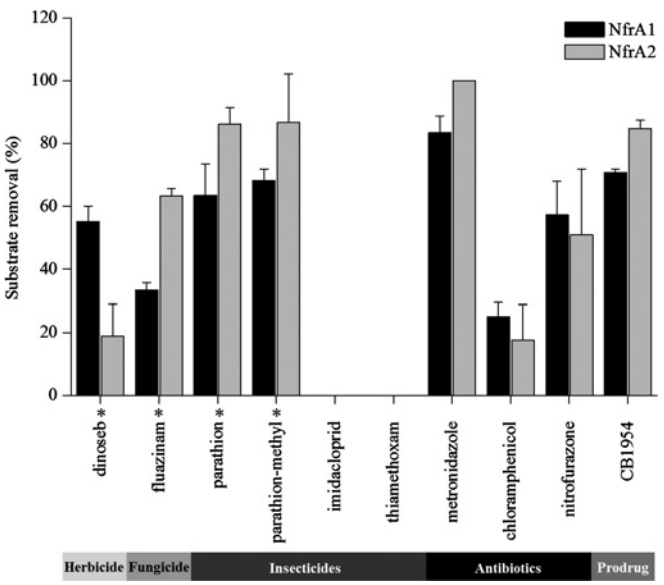

Figure 3 Mes11 NfrA1 and NfrA2/YcnD NR activities on various nitro compounds determined by HPLC

The incubations were carried out for 1 h at the optimal pH (6) and temperature (25 °C) in NPB with 1.8 μM NfrA1 or NfrA2/YcnD and 400 μM substrate except in the case of (*) dinoseb and methyl-parathion (200 μM), parathion (80 μM) and fluazinam (5 μM) due to their lower solubilities. The results are reported as means ± S.D. ($n = 3$).

NfrA1 for nitro reduction of both substrates when NADH was used as the electron donor.

The type I NRs previously described possess a broad substrate specificity [36]. It is interesting that both NfrA1 and NfrA2/YcnD could also transform various nitro compounds, indicating that they do not present substrate specificity (Figure 3 and see Supplementary Figure S3). The only exceptions were two neonicotinoid insecticides (imidacloprid and thiamethoxam) for which the nitro group is not aromatic.

Surprisingly, they were able to reduce nitro groups of the herbicide dinoseb and the fungicide fluazinam, even if, until now, these biotransformations have been described only in anaerobic conditions [37–40]. NfrA1 and NfrA2/YcnD of *B. megaterium* could also reduce the nitro group of the parathion-methyl and parathion insecticides in high proportions (Figure 3), although only hydrolase and esterase activities have been described for the first transformation step of these molecules [41–44].

The bacterial NRs have already been described as being involved in the modulation of antibiotic resistance, mainly against metronidazole [36]. It is interesting that antibiotics such as metronidazole, chloramphenicol and nitrofurazone can also be substrates for Mes11 NfrA1 and NfrA2/YcnD (Figure 3).

© 2016 Authors; published by Portland Press Limited

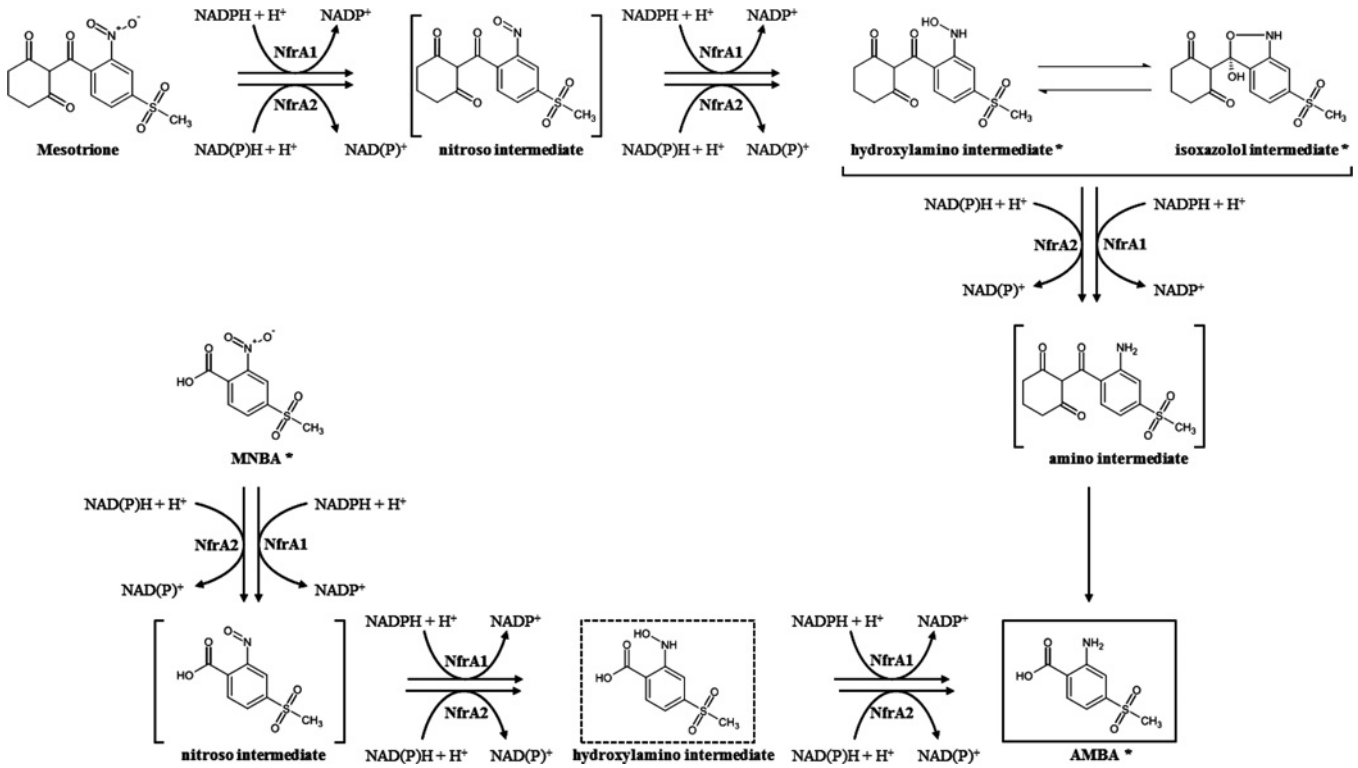

Figure 4 Proposed scheme of mesotrione and MNBA biotransformation by NfrA1 and NfrA2/YcnD

The brackets indicate the undetected intermediates during enzymatic assays. The major end-product of mesotrione (square box) and MNBA (dotted box) are indicated. *Mesotrione transformation products also detected in *B. megaterium* Mes11 resting cell experiments [11] (the present study).

Metronidazole and nitrofurazone are activated when their nitro group is reduced whereas chloramphenicol is more active than its hydroxylamino and amino derivatives [36,45]. The high metronidazole and nitrofurazone, and low chloramphenicol, transformation rates by Mes11 NRs (Figure 3) could thus explain the sensitivity of the Mes11 strain to these three molecules (results not shown).

Furthermore, the two Mes11 NRs could also reduce the prodrug CB1954, suggesting that they could be used as prodrug activators (Figure 3). Indeed, the NRs have already been used in cancer therapy to activate a nitro-substituted prodrug into a cytotoxic hydroxylamino derivative by reduction of the nitro group [36,46].

Biotransformation of mesotrione and MNBA by NfrA1 and NfrA2/YcnD

The biotransformation of mesotrione and MNBA by NfrA1 and NfrA2/YcnD was investigated in more detail, showing the formation of nitro-reduced products previously described with the *B. megaterium* Mes11 strain [11] (Figure 4).

The reduction of the nitro group of mesotrione by Mes11 NfrA1 and NfrA2/YcnD required three molecules of NAD(P)H cofactor, which is consistent with the stoichiometry of the reduction of nitro compounds [29]. Three mesotrione nitro-reduced products were detected and identified by UV, ^{1}H NMR and LC–MS as previously described [13]: the hydroxylamino derivative in equilibrium with the cyclized isoxazolol intermediate and AMBA, the final and accumulating metabolite also observed with the Mes11 strain (Figures 4 and 5). The nitroso intermediate was not detected, probably due to the higher reaction rate of the second two-electron transfer compared with the first one. This phenomenon has already been described with other NRs [47,48]. The amino intermediate, theoretically formed as the NR end-product of the complete reduction of the mesotrione nitro group, was not identified in our experiments, probably due to its spontaneous hydrolysis leading to the formation of AMBA under the slightly acidic conditions used in the enzymatic assay (pH 6). It could be explained by replacing the deactivating mesomeric effect of the nitro group by the activating one of the amino group. Moreover, the involvement of two enzymes to transform mesotrione into AMBA has been previously hypothesized in a resting cell experiment [11], one enzyme being responsible for the nitro reduction and another for the oxidative cleavage of the molecule. However, our *in vitro* enzymatic assays with only Mes11 NR lead to the end-product AMBA, suggesting that the second step is probably an abiotic one and that mesotrione could be completely transformed to the final metabolite by only one type of enzyme in Mes11 culture experiments. The quantitative time-course transformation of the mesotrione and mass balance calculation (Figures 5A and 5C) correlate with the data previously observed in *B. megaterium* Mes11 resting cell experiments [11].

Similar results were obtained with MNBA as the electron acceptor, with no detection of a nitroso intermediate. Two MNBA nitro-reduction products were detected: the hydroxylamino derivative (major proportion) identified by UV (specific band at 355 nm [49,50] and LC–(−)ESI–MS (high-resolution MS) ($m/z = 230.0118$, $C_8H_8NO_5S^-$ with a mass error of 0.5 mDa), and AMBA (minor proportion), identified by comparison of the different spectroscopic data with a standard; this showed the capacity of NfrA1 and NfrA2/YcnD to reduce the nitro groups *via* the common mechanism of type I NRs (Figures 4 and 5).

© 2016 Authors; published by Portland Press Limited

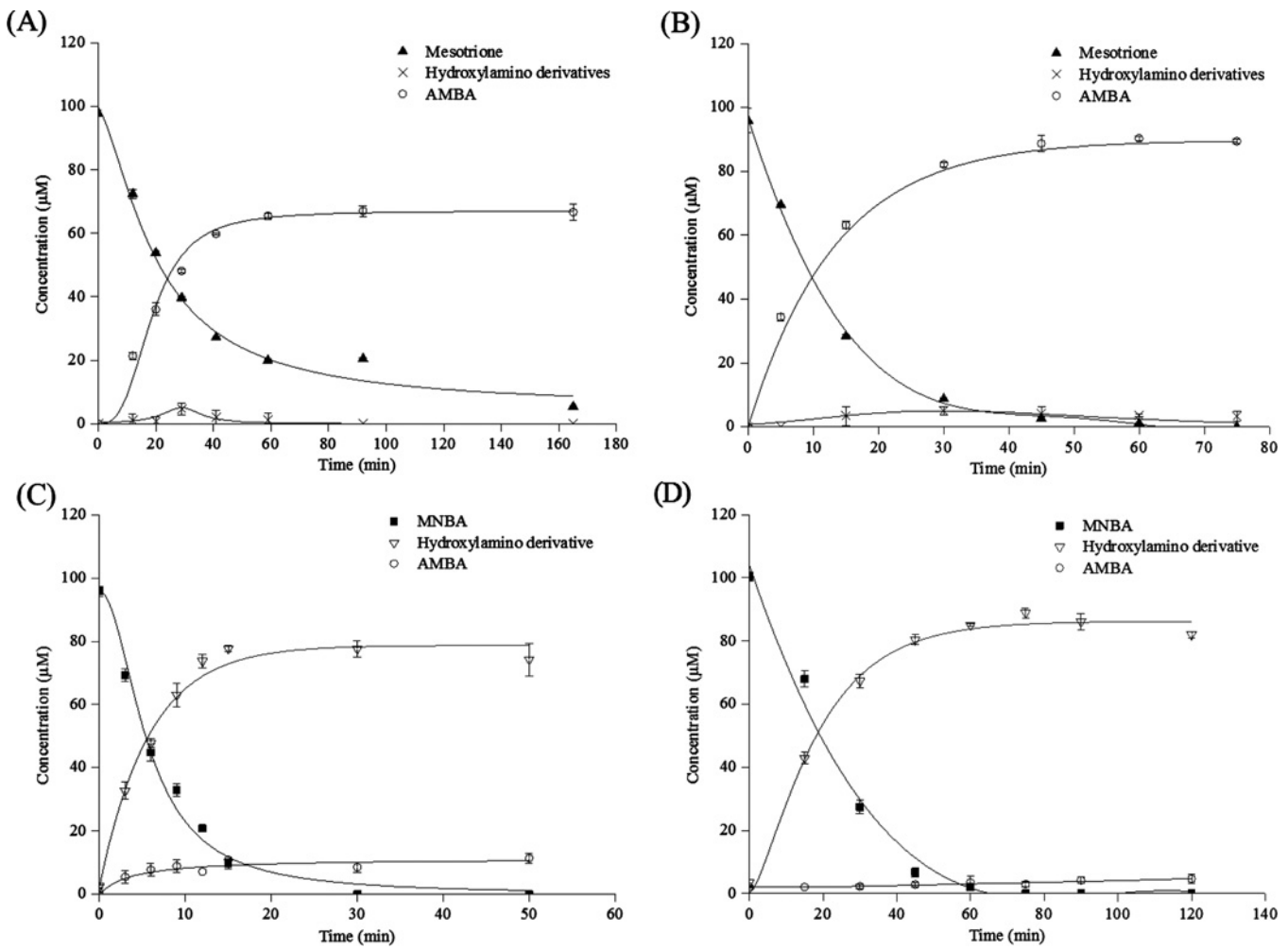

Figure 5 Quantification of mesotrione and MNBA

(**A** and **B**) Quantification of mesotrione and (**C** and **D**) MNBA during incubation with (**A** and **C**) NfrA1 and (**B** and **D**) NfrA2/YcnD. The incubations were carried out in NPB at optimal pH (6) and temperature (25 °C), with 2.4 μM NfrA1 or NfrA2/YcnD, 100 μM mesotrione or MNBA, and 400 μM NADPH. The final concentrations (μM) were: (**A**) mesotrione 3.8 $\pm$ 0.1, hydroxylamino derivatives 5.9 $\pm$ 3.8 and AMBA 67.7 $\pm$ 1.3; (**B**) mesotrione 0.0 $\pm$ 0.0, hydroxylamino derivatives 3.3 $\pm$ 1.7 and AMBA 89.4 $\pm$ 0.7; (**C**) MNBA 0.0 $\pm$ 0.0, hydroxylamino derivative 83.9 $\pm$ 2.7 and AMBA 10.6 $\pm$ 1.5; and (**D**) MNBA 0.0 $\pm$ 0.0, hydroxylamino derivative 76.1 $\pm$ 1.5 and AMBA 8.6 $\pm$ 1.5. The results are reported as means $\pm$ S.D. ($n = 3$).

The quantitative time-course transformation of the MNBA and mass balance calculation are shown in Figures 5(B) and 5(D). The presence of an MNBA hydroxylamino intermediate was not reported in experiments with Mes11 resting cell cultures, probably due to its rapid transformation into AMBA under *in situ* conditions.

Influence of mesotrione on *nfr*A1 and *nfr*A2/*ycn*D gene expression levels in *B. megaterium* Mes11

We investigated the *nfr*A1 and *nfr*A2/*ycn*D gene expression levels in the presence of mesotrione to gain insight into the possible role of these enzymes in Mes11 resting cell experiments. A similar growth of Mes11 was observed in tryptone soya medium supplemented or not with mesotrione. The disappearance of mesotrione (52.7 $\pm$ 2.6 % in 15 h) was measured, together with the up-regulation of *nfr*A1 (2 $\pm$ 0.5-fold) and *nfr*A2/*ycn*D (5.5 $\pm$ 1-fold) genes, suggesting that both genes are mesotrione-inducible. These results suggest that NfrA1 and NfrA2/YcnD could be involved in mesotrione biotransformation in *B. megaterium* Mes11 cells. However, the physiological involvement of these two enzymes in mesotrione and MNBA transformation could not be proved because all of the transformation methods used ($CaCl_2$ transformation, electroporation, protoplast transformation, conjugation) to obtain NfrA mutants failed, thus preventing us from ascertaining their role in *B. megaterium* Mes11.

Conclusions

The identification of NfsA FRP enzymes in three genera (*Bacillus*, *Pantoea* and *Escherichia*) containing strains able to biotransform mesotrione into hydroxylamino intermediates and AMBA [9] strongly suggests that there could be a common mesotrione-biotransformation process involving this enzyme family, allowing the development of a specific biomarker of mesotrione biotransformation in various ecosystems.

The broad activity spectrum of both Mes11 NRs on various nitro compounds such as antibiotics, pesticides and prodrugs could lead to their potential use in biotechnology, as already described for other NRs, to develop, for example, *in situ* electrochemical biosensors for the detection of nitro-aromatic compounds, bioremediation processes or enzyme prodrug therapy applications. Such investigations are in progress in our laboratory.

© 2016 Authors; published by Portland Press Limited

AUTHOR CONTRIBUTION

Isabelle Batisson carried out the screening of genes and primer design. Louis Carles, Muriel Joly and Isabelle Batisson carried out the design of experiments, protein expression and purification for kinetic assays, the screening of protein activities and functional analyses, as well as interpretation of the results. Louis Carles and Muriel Joly carried out the gene expression analyses. Pascale Besse-Hoggan carried out the chemical analyses and metabolite identification. Armelle Vigouroux and Solange Moréra carried out the protein purification for crystallization, the crystallization itself and the structural analyses. All authors contributed to the writing of the paper, with Louis Carles, Pascale Besse-Hoggan and Isabelle Batisson making major contributions.

ACKNOWLEDGEMENTS

We thank Egon Heuson and Franck Charmantray for helpful advice and suggestions and Philip Hoggan for English reviewing. We acknowledge SOLEIL for provision of Synchrotron radiation facilities (proposal ID 20140774) in using beamlines Proxima 1 and 2.

FUNDING

This work was supported by the Agence Nationale de la Recherche [grant number ANR-13-CESA-0002 TRICETOX] (programme CESA), the Région Auvergne, the French Ministry for Higher Education and Research and the European Regional Development Fund. This work has benefited from the I2BC crystallization platform, supported by French Infrastructure for Integrated Structural Biology [grant number FRISBI ANR-10-INSB-05–01].

REFERENCES

1 Cantrell, C.L., Dayan, F.E. and Duke, S.O. (2012) Natural products as sources for new pesticides. J. Nat. Prod. **75**, 1231–1242 CrossRef PubMed
2 Duke, S., Owens, D. and Dayan, F. (2014) The growing need for biochemical bioherbicides. In ACS Symposium Series, pp. 31–43, American Chemical Society, Washington CrossRef
3 Bonnet, J.L., Bonnemoy, F., Dusser, M. and Bohatier, J. (2008) Toxicity assessment of the herbicides sulcotrione and mesotrione toward two reference environmental microorganisms: *Tetrahymena pyriformis* and *Vibrio fischeri*. Arch. Environ. Contam. Toxicol. **55**, 576–583 CrossRef PubMed
4 Barchanska, H. (2012) Triketones herbicides: expectations and risk. In Advances in chemistry research (Taylor, J.C., ed.), pp. 243–264, Nova Science Publishers, New York
5 Chaabane, H., Vulliet, Calvayrac, E., Coste, C., -M., C. and Cooper, J.-F. (2008) Behaviour of sulcotrione and mesotrione in two soils. Pest Manag. Sci. **64**, 86–93 CrossRef PubMed
6 Dyson, J.S., Beulke, S., Brown, C.D. and Lane, M.C.G. (2002) Adsorption and degradation of the weak acid mesotrione in soil and environmental fate implications. J. Environ. Qual. **31**, 613–618 CrossRef PubMed
7 Alferness, P. and Wiebe, L. (2002) Determination of mesotrione residues and metabolites in crops, soil, and water by liquid chromatography with fluorescence detection. J. Agric. Food Chem. **50**, 3926–3934 CrossRef PubMed
8 Durand, S., Amato, P., Sancelme, M., Delort, A.-M., Combourieu, B. and Besse-Hoggan, P. (2006) First isolation and characterization of a bacterial strain that biotransforms the herbicide mesotrione. Lett. Appl. Microbiol. **43**, 222–228 CrossRef PubMed
9 Youness, M. (2013) Impact de la Formulation et du Mélange de Deux Pesticides (Mésotrione et Tébuconazole) sur Leur Biodégradation et la Croissance de Microorganismes. Ph.D. Thesis, Université Blaise Pascal, Clermont-Ferrand, France
10 Liu, J., Chen, S., Ding, J., Xiao, Y., Han, H. and Zhong, G. (2015) Sugarcane bagasse as support for immobilization of *Bacillus pumilus* HZ-2 and its use in bioremediation of mesotrione-contaminated soils. Appl. Microbiol. Biotechnol. **99**, 10839–10851 CrossRef PubMed
11 Batisson, I., Crouzet, O., Besse-Hoggan, P., Sancelme, M., Mangot, J.-F., Mallet, C. and Bohatier, J. (2009) Isolation and characterization of mesotrione-degrading *Bacillus* sp. from soil. Environ. Pollut. **157**, 1195–1201 CrossRef PubMed
12 Romdhane, S., Devers-Lamrani, M., Martin-Laurent, F., Calvayrac, C., Rocaboy-Faquet, E., Riboul, D., Cooper, J.-F. and Barthelmebs, L. (2016) Isolation and characterization of *Bradyrhizobium* sp. SR1 degrading two β-triketone herbicides. Environ. Sci. Pollut. Res. Int. **23**, 4138–4148 PubMed
13 Durand, S., Sancelme, M., Besse-Hoggan, P. and Combourieu, B. (2010) Biodegradation pathway of mesotrione: Complementarities of NMR, LC-NMR and LC-MS for qualitative and quantitative metabolic profiling. Chemosphere **81**, 372–380 CrossRef PubMed
14 Bardot, C., Besse-Hoggan, P., Carles, L., Le Gall, M., Clary, G., Chafey, P., Federici, C., Broussard, C. and Batisson, I. (2015) How the edaphic *Bacillus megaterium* strain Mes11 adapts its metabolism to the herbicide mesotrione pressure. Environ. Pollut. **199**, 198–208 CrossRef PubMed
15 Peterson, F.J., Mason, R.P., Hovsepian, J. and Holtzman, J.L. (1979) Oxygen-sensitive and-insensitive nitroreduction by *Escherichia coli* and rat hepatic microsomes. J. Biol. Chem. **254**, 4009–4014 PubMed
16 Bryant, D.W., McCalla, D.R., Leeksma, M. and Laneuville, P. (1981) Type I nitroreductases of *Escherichia coli*. Can. J. Microbiol. **27**, 81–86 CrossRef PubMed
17 Mason, R.P. and Holtzman, J.L. (1975) The role of catalytic superoxide formation in the O_2 inhibition of nitroreductase. Biochem. Biophys. Res. Commun. **67**, 1267–1274 CrossRef PubMed
18 Borrel, G., Lehours, A.-C., Crouzet, O., Jézéquel, D., Rockne, K., Kulczak, A., Duffaud, E., Joblin, K. and Fonty, G. (2012) Stratification of archaea in the deep sediments of a freshwater meromictic lake: vertical shift from methanogenic to uncultured archaeal lineages. PLoS One **7**, e43346 CrossRef PubMed
19 Bers, K., Batisson, I., Proost, P., Wattiez, R., De Mot, R. and Springael, D. (2013) HylA, an alternative hydrolase for initiation of catabolism of the phenylurea herbicide linuron in *Variovorax* sp. strains. Appl. Environ. Microbiol. **79**, 5258–5263 CrossRef PubMed
20 Kabsch, W. (2010) Xds. Acta Crystallogr. D Biol. Crystallogr. **66**, 125–132 CrossRef PubMed
21 Karplus, P.A. and Diederichs, K. (2012) Linking crystallographic model and data quality. Science **336**, 1030–1033 CrossRef PubMed
22 McCoy, A.J., Grosse-Kunstleve, R.W., Adams, P.D., Winn, M.D., Storoni, L.C. and Read, R.J. (2007) Phaser crystallographic software. J. Appl. Crystallogr. **40**, 658–674 CrossRef PubMed
23 Cortial, S., Chaignon, P., Iorga, B.I., Aymerich, S., Truan, G., Gueguen-Chaignon, V., Meyer, P., Moréra, S. and Ouazzani, J. (2010) NADH oxidase activity of *Bacillus subtilis* nitroreductase NfrA1: insight into its biological role. FEBS Lett. **584**, 3916–3922 CrossRef PubMed
24 Morokutti, A., Lyskowski, A., Sollner, S., Pointner, E., Fitzpatrick, T.B., Kratky, C., Gruber, K. and Macheroux, P. (2005) Structure and function of YcnD from *Bacillus subtilis*, a flavin-containing oxidoreductase. Biochemistry **44**, 13724–13733 CrossRef PubMed
25 Blanc, E., Roversi, P., Vonrhein, C., Flensburg, C., Lea, S.M. and Bricogne, G. (2004) Refinement of severely incomplete structures with maximum likelihood in BUSTER-TNT. Acta Crystallogr. D Biol. Crystallogr. **60**, 2210–2221 CrossRef PubMed
26 Emsley, P. and Cowtan, K. (2004) Coot: model-building tools for molecular graphics. Acta Crystallogr. D Biol. Crystallogr. **60**, 2126–2132 CrossRef PubMed
27 Dugat-Bony, E., Missaoui, M., Peyretaillade, E., Biderre-Petit, C., Bouzid, O., Gouinaud, C., Hill, D. and Peyret, P. (2011) HiSpOD: probe design for functional DNA microarrays. Bioinformatics **27**, 641–648 CrossRef PubMed
28 Durand, S., Légeret, B., Martin, A.-S., Sancelme, M., Delort, A.-M., Besse-Hoggan, P. and Combourieu, B. (2006) Biotransformation of the triketone herbicide mesotrione by a *Bacillus* strain. Metabolite profiling using liquid chromatography/electrospray ionization quadrupole time-of-flight mass spectrometry. Rapid Commun. Mass Spectrom. **20**, 2603–2613 CrossRef PubMed
29 Roldán, M.D., Pérez-Reinado, E., Castillo, F. and Moreno-Vivián, C. (2008) Reduction of polynitroaromatic compounds: the bacterial nitroreductases. FEMS Microbiol. Rev. **32**, 474–500 CrossRef PubMed
30 Gouet, P., Courcelle, E., Stuart, D.I. and Metoz, F. (1999) ESPript: analysis of multiple sequence alignments in PostScript. Bioinformatics **15**, 305–308 CrossRef PubMed
31 Zenno, S., Kobori, T., Tanokura, M. and Saigo, K. (1998) Purification and characterization of NfrA1, a *Bacillus subtilis* nitro/flavin reductase capable of interacting with the bacterial luciferase. Biosci. Biotechnol. Biochem. **62**, 1978–1987 CrossRef PubMed
32 Kim, H.-Y. and Song, H.-G. (2005) Purification and characterization of NAD(P)H-dependent nitroreductase I from *Klebsiella* sp. C1 and enzymatic transformation of 2,4,6-trinitrotoluene. Appl. Microbiol. Biotechnol. **68**, 766–773 CrossRef PubMed
33 Kim, Y.-H., Song, W.-S., Go, H., Cha, C.-J., Lee, C., Yu, M.-H., Lau, P.C.K. and Lee, K. (2013) 2-Nitrobenzoate 2-nitroreductase (NbaA) switches its substrate specificity from 2-nitrobenzoic acid to 2,4-dinitrobenzoic acid under oxidizing conditions. J. Bacteriol. **195**, 180–192 CrossRef PubMed
34 Prosser, G.A., Copp, J.N., Mowday, A.M., Guise, C.P., Syddall, S.P., Williams, E.M., Horvat, C.N., Swe, P.M., Ashoorzadeh, A., Denny, W.A. et al. (2013) Creation and screening of a multi-family bacterial oxidoreductase library to discover novel nitroreductases that efficiently activate the bioreductive prodrugs CB1954 and PR-104A. Biochem. Pharmacol. **85**, 1091–1103 CrossRef PubMed
35 Zenno, S., Koike, H., Kumar, A.N., Jayaraman, R., Tanokura, M. and Saigo, K. (1996) Biochemical characterization of NfsA, the *Escherichia coli* major nitroreductase exhibiting a high amino acid sequence homology to Frp, a *Vibrio harveyi* flavin oxidoreductase. J. Bacteriol. **178**, 4508–4514 PubMed
36 De Oliveira, I.M., Bonatto, D. and Henriques, J.A.P. (2010) Nitroreductases: enzymes with environmental, biotechnological and clinical importance. Reactions **3**, 6

© 2016 Authors; published by Portland Press Limited

37 Hammill, T.B. and Crawford, R.L. (1996) Degradation of 2-*sec*-butyl-4, 6-dinitrophenol (dinoseb) by *Clostridium bifermentans* KMR-1. Appl. Environ. Microbiol. **62**, 1842–1846 PubMed
38 Hutson, D.H. (1998) Metabolic Pathways of Agrochemicals: Herbicides and Plant Growth Regulators, Royal Society of Chemistry, Cambridge
39 Kaake, R.H., Crawford, D.L. and Crawford, R.L. (1995) Biodegradation of the nitroaromatic herbicide dinoseb (2-*sec*-butyl-4, 6-dinitrophenol) under reducing conditions. Biodegradation **6**, 329–337 CrossRef PubMed
40 European Food Safety Authority (2008) Conclusion Regarding the Peer Review of the Pesticide Risk Assessment of the Active Substance Fluazinam. EFSA Scientific Report 137
41 Serdar, C.M. and Gibson, D.T. (1985) Enzymatic hydrolysis of organophosphates: cloning and expression of a parathion hydrolase gene from *Pseudomonas diminuta*. Bio/Technology **3**, 567–571 CrossRef
42 Mulbry, W.W. and Karns, J.S. (1989) Purification and characterization of three parathion hydrolases from gram-negative bacterial strains. Appl. Environ. Microbiol. **55**, 289–293 PubMed
43 Alvarenga, N., Birolli, W.G., Seleghim, M.H.R. and Porto, A.L.M. (2014) Biodegradation of methyl parathion by whole cells of marine-derived fungi *Aspergillus sydowii* and *Penicillium decaturense*. Chemosphere **117**, 47–52 CrossRef PubMed
44 Hao, J., Liu, J. and Sun, M. (2014) Identification of a marine *Bacillus* strain C5 and parathion-methyl degradation characteristics of the extracellular esterase B1. Biomed. Res. Int. **2014**, 863094 PubMed
45 Smith, A.L., Erwin, A.L., Kline, T., Unrath, W.C.T., Nelson, K., Weber, A. and Howald, W.N. (2007) Chloramphenicol is a substrate for a novel nitroreductase pathway in *Haemophilus influenzae*. Antimicrob. Agents Chemother. **51**, 2820–2829 CrossRef PubMed
46 Williams, E.M., Little, R.F., Mowday, A.M., Rich, M.H., Chan-Hyams, J.V.E., Copp, J.N., Smaill, J.B., Patterson, A.V. and Ackerley, D.F. (2015) Nitroreductase gene-directed enzyme prodrug therapy: insights and advances toward clinical utility. Biochem. J. **471**, 131–153 CrossRef PubMed
47 Koder, R.L., Haynes, C.A., Rodgers, M.E., Rodgers, D.W. and Miller, A.-F. (2002) Flavin thermodynamics explain the oxygen insensitivity of enteric nitroreductases. Biochemistry **41**, 14197–14205 CrossRef PubMed
48 Race, P.R., Lovering, A.L., Green, R.M., Ossor, A., White, S.A., Searle, P.F., Wrighton, C.J. and Hyde, E.I. (2005) Structural and mechanistic studies of *Escherichia coli* nitroreductase with the antibiotic nitrofurazone. J. Biol. Chem. **280**, 13256–13264 CrossRef PubMed
49 Barth, A., Corrie, J.E.T., Gradwell, M.J., Maeda, Y., Mäntele, W., Meier, T. and Trentham, D.R. (1997) Time-resolved infrared spectroscopy of intermediates and products from photolysis of 1-(2-nitrophenyl)ethyl phosphates: reaction of the 2-nitrosoacetophenone byproduct with thiols. J. Am. Chem. Soc. **119**, 4149–4159 CrossRef
50 Uncuta, C., Tudose, A., Caproiu, M.T., Udrea, S. and Roussel, C. (2003) Correction to withdrawn article. Cyclization products of δ-oxo-α,β-unsaturated ketoxime during reaction with hydrochloric acid in anhydrous diethyl ether. Eur. J. Org. Chem. **2003**, 1789–1795 CrossRef

Received 12 January 2016/11 March 2016; accepted 22 March 2016
Accepted Manuscript online 22 March 2016, doi:10.1042/BJ20151366

© 2016 Authors; published by Portland Press Limited